

Real-Space Renormalization Group for Langevin Dynamics in Absence of Translational Invariance

Achille Giacometti,¹ Amos Maritan,² Flavio Toigo,³ and Jayanth R. Banavar⁴

Received June 17, 1994; final November 8, 1994

A novel exact dynamical real-space renormalization group for a Langevin equation derivable from a Euclidean Gaussian action is presented. It is demonstrated rigorously that an algebraic temporal law holds for the Green function on arbitrary structures of infinite extent. In the case of fractals it is shown on specific examples that two different fixed points are found, at variance with periodic structures. Connection with the growth dynamics of interfaces is also discussed.

KEY WORDS: Random processes; surface growth; renormalization group; fractals.

1. INTRODUCTION

Dynamical renormalization group (DRG) analyses of the critical dynamics of statistical mechanics models has a long history^{(4), 5} with virtually all studies on regular translationally invariant structures. These approaches were, both in real and in momentum space, of a perturbative nature; in contrast, the principal aim of the present paper is the implementation of

¹ Dipartimento di Fisica dell'Università di Padova, 35100 Padova, Italy. Present address: Institut für Festkörperforschung der Kernforschungsanlage, D-52425, Jülich, Germany.

² Dipartimento di Fisica dell'Università and Istituto Nazionale di Fisica Nucleare, Sezione di Padova, 35100 Padova, Italy.

³ Dipartimento di Fisica dell'Università and Istituto Nazionale di Fisica della Materia INFM, 35100 Padova, Italy.

⁴ Department of Physics and Center for Materials Physics, 104 Davey Laboratory, Pennsylvania State University, University Park, Pennsylvania 16802.

⁵ See the review article by Hohenberg and Halperin⁽¹⁾; see also Ma.⁽²⁾ For a review of real-space dynamical RG for the time evolution operator see Mazenko.⁽³⁾

an *exact* approach, in real space, for the dynamics occurring on fractal structures.

Consider a system described by a Hamiltonian (or action) $H(\{\varphi\})$ with the field variables φ_x defined on the lattice sites x . The simplest Langevin⁽¹⁾ dynamics leading to equilibrium with the correct Boltzmann weight $\exp[-H(\{\varphi\})]$ is⁶

$$\frac{\partial \varphi_x(t)}{\partial t} = -\frac{\delta H(\{\varphi\})}{\delta \varphi_x} + \eta_x(t) \quad (1)$$

The temperature has been absorbed in the definition of H . The stochastic noise $\eta_x(t)$ is chosen from a Gaussian distribution

$$\mathcal{P}(\{\eta(t)\}) = \mathcal{N}^{-t} \exp\left(-\sum_x \int dt \frac{\eta_x^2(\tau)}{4D}\right) \quad (2)$$

(\mathcal{N}^{-1} is a normalization factor) which has a zero average and variance $\langle \eta_x(t) \eta_y(t') \rangle = 2D \delta_{x,y} \delta(t-t')$.

We consider the simplest possible choice of the Hamiltonian $H(\{\varphi\})$, the Gaussian model:

$$H(\{\varphi\}) = \sum_x \frac{a_x}{2} \varphi_x^2 - \sum_{\langle xy \rangle} \varphi_x \varphi_y \quad (3)$$

where a_x depends on temperature and the scale of φ_x is such that the second term in (3), i.e., the sum over nearest-neighbor sites, has coefficient 1.

Besides being the starting point of more complicated models, the Gaussian model is related to many physical situations such as the properties of an ideal polymer in solution,⁽⁵⁾ diffusion processes, and the growth dynamics of interfaces.⁽⁶⁾ Indeed, if $a_x = k^{-1}$ for any x , then the Hamiltonian (3) describes the equilibrium properties of an ideal linear polymer in solution with a monomer fugacity equal to k . If $a_x = z_x$, the coordination number of site x , the Hamiltonian (3) can be rewritten as

$$H = \frac{1}{2} \sum_{\langle x,y \rangle} (\varphi_x - \varphi_y)^2 \quad (4)$$

and it is related to the diffusion process known as the *ant in the labyrinth* (ref. 5; for review see, e.g., ref. 7).

If φ_x represents the height of an interface above the substrate point x (in the solid-on-solid approximation), then Eq. (3) can be interpreted as

⁶ A clear presentation of this point of view is ref. 2.

the energy of an interface and the Langevin equation (1) describes its dynamics. In a regular (hyper)cubic lattice this is known as the Edwards–Wilkinson model for interface dynamics.⁽⁶⁾

We shall show, in specific examples, that in the presence of nontranslational structures (such as fractals) even the simple model (3) gives rise to interesting behaviors. Specifically, we will show that *two* different fixed points are present, unlike in structures with translational invariance, where they collapse to the same fixed point. Some of the results presented here appeared in ref. 8.

The paper is organized as follows. In Section 2 we introduce the DRG technique for this problem first in the simple case of a one-dimensional lattice and then in a situation in which the couplings have a hierarchical structure. In Section 3 the nontrivial cases of fractal structures with uniform and nonuniform coordination number are analyzed. In the latter case it will be shown that there is an additional universality class. Section 4 contains both rigorous and heuristic arguments on a general network and for a nonlinear case. The heuristic arguments are then checked by the numerical analysis of Section 5. Finally in Section 6 some closing conclusions are presented.

2. ONE-DIMENSIONAL LATTICE

We shall start with the simple case of a one-dimensional lattice. After a pedagogical example with uniform couplings, we will turn to a nontrivial example. In the latter case only DRG allows us to obtain the asymptotic solution.

2.1. Uniform Couplings

Let us start with a one-dimensional case in order to show how the method works. Equation (1) for the Hamiltonian (3) with $a_x = a$ has then the form

$$\frac{\partial \varphi_x(t)}{\partial t} = (\varphi_{x-1}(t) + \varphi_{x+1}(t) - a\varphi_x(t)) + \eta_x(t) \quad (5)$$

It is immediately clear that if we were to choose uncorrelated noise, decimation would produce correlation between the nearest-neighbor noises. We thus assume a nearest-neighbor correlation to start with, that is,

$$\langle \eta_x(t_1) \eta_y(t_2) \rangle = 2D_{x,y} \delta(t_1 - t_2) \quad (6)$$

where $D_{x,y} = D_0 \delta_{x,y} + D_1 \delta_{x \pm 1,y}$. As usual it is convenient to work in (time) Fourier space:

$$\alpha \hat{\phi}_x(\omega) = \hat{\phi}_{x-1}(\omega) + \hat{\phi}_{x+1}(\omega) + \hat{\eta}_x(\omega) \tag{7}$$

where

$$f_x(t) \equiv \int_{-\infty}^{+\infty} \frac{d\omega}{2\pi} e^{-i\omega t} \hat{f}_x(\omega) \tag{8}$$

and $\alpha = a - i\omega$.

Upon decimation of (e.g.) the odd sites in favor of the even ones [i.e., solving Eq. (7) for $\hat{\phi}_{2x \pm 1}$ in terms of $\hat{\phi}_{2x}$ and $\hat{\phi}_{2x \pm 2}$], we get an equation for the surviving (even) sites:

$$(\alpha^2 - 2) \frac{\hat{\phi}_{2x}(\omega)}{\alpha} = \frac{\hat{\phi}_{2x-2}(\omega) + \hat{\phi}_{2x+2}(\omega)}{\alpha} + \hat{\zeta}_{2x}(\omega) \tag{9}$$

where we have defined a new noise $\hat{\zeta}_x(\omega)$ as

$$\hat{\zeta}_{2x}(\omega) = \hat{\eta}_{2x}(\omega) + \frac{\hat{\eta}_{2x-1}(\omega) + \hat{\eta}_{2x+1}(\omega)}{\alpha} \tag{10}$$

which is correlated as

$$\langle \hat{\zeta}_x(\omega_1) \hat{\zeta}_y(\omega_2) \rangle = 2\bar{D}_{x,y}(2\pi) \delta(\omega_1 + \omega_2) \tag{11}$$

where as before $\bar{D}_{x,y} = \bar{D}_0 \delta_{x,y} + \bar{D}_1 \delta_{x \pm 1,y}$ and

$$\bar{D}_0 = D_0 \left(1 + \frac{2}{\alpha^2} \right) + D_1 \frac{4}{\alpha} \tag{12a}$$

$$\bar{D}_1 = D_0 \frac{1}{\alpha^2} + D_1 \frac{2}{\alpha} \tag{12b}$$

Therefore the new noise keeps the same correlation as the original one and, being a linear combination of Gaussian noises, is itself a Gaussian noise. With the redefinitions

$$\hat{\phi}_{2x}(\alpha, D) = \alpha A \hat{\phi}_x(\alpha', D') \tag{13a}$$

$$\alpha' = \alpha^2 - 2 \tag{13b}$$

$$\hat{\zeta}_{2x} = A \hat{\eta}'_{x'} \tag{13c}$$

the Langevin equation preserves its original form. The static recursion relation for a is obtainable from (13b) for $\omega = 0$, i.e.,

$$a' = a^2 - 2 \tag{14}$$

from which the recursion equation for ω is derivable. Indeed if $\alpha = a - i\omega$, then $\alpha' = a' - i\omega'$ with

$$\omega' = 2a\omega - i\omega^2 \tag{15}$$

The variance of the new noise is $\langle \hat{\eta}_x(\omega'_1) \hat{\eta}_y(\omega'_2) \rangle = 2D'_{x,y}(2\pi) \delta(\omega'_1 + \omega'_2)$ with $D'(\omega') = T(\omega) \cdot D(\omega)$. Here we have defined the 1×2 matrix

$$D = \begin{pmatrix} D_0 \\ D_1 \end{pmatrix}$$

and T is the transmission matrix which, in the long-time limit $\omega \rightarrow 0$, becomes

$$T = \frac{2a}{A^2} \begin{pmatrix} 1 + 2/a^2 & 4/a \\ 1/a^2 & 2/a \end{pmatrix} \tag{16}$$

It is important to note that the amplitude A , which is always allowed since it drops out from the final equations, is determined by the fixed-point condition on D . The critical fixed point of Eq. (14) is $a^* = 2$ [model (3) in 1d is meaningful only for $a \geq 2$]. Since we are interested in critical dynamics, we will put $a = a^* = 2$ in what follows. By setting the determinant of the system giving the fixed point for the matrix D equal to zero one obtains two solutions (two lines of fixed points corresponding to fixed ratio D_0/D_1) associated respectively with $A^* = 2^{1/2}$ and $A^* = 2^{3/2}$. It is easy to see that the first choice leads to an unstable solution, while the second results in a stable one. Indeed, let Λ_+ and Λ_- be the two eigenvalues of the transmission matrix T , and u_+ and u_- the corresponding eigenvectors. Then if we start with an initial state D

$$D = c_+ u_+ + c_- u_- \tag{17}$$

(c_{\pm} being the coefficients of the expansion in the basis of eigenvectors), upon iteration of the RG transformation, the variance grows unbounded with the choice $A^* = 2^{1/2}$, while it is driven toward a stable fixed point $D^* = c_+ u_+$ with the choice $A^* = 2^{3/2}$.

We now have the means to compute the critical exponents of interest. From Eq. (13a) we have, at the stable fixed point, for a generic scaling factor $b > 1$,

$$\hat{\phi}_{hx}(\omega, D^*) = b^\phi \hat{\phi}_x(b^z \omega, D^*) \quad (18)$$

where $\phi = 5/2$, $z = 2$ is the dynamical exponent z , and we have written $\hat{\phi}(\omega, D)$ instead of $\hat{\phi}(2 - i\omega, D)$. The exponent ϕ can be related to the scaling of the two-point correlation function:

$$G_{x,y}(t_1, t_2) = \langle \varphi_x(t_1) \varphi_y(t_2) \rangle \quad (19)$$

where the average is over noise configurations. Using Eq. (18), we get

$$G_{hx,0}(t_1, t_2) = b^{2(\phi - z)} G_{x,0}\left(\frac{t_1}{b^z}, \frac{t_2}{b^z}\right) \quad (20)$$

The properties of the *equal-time* correlation function can now be easily derived. If we define the function $W^2(L, t) \equiv G_{L,0}(t, t)$, we end up with the following scaling form:

$$W(L, t) = L^\alpha F\left(\frac{t}{L^z}\right) \quad (21)$$

with $\alpha = \phi - z = 1/2$ and $z = 2$.

A few comments are in order. If φ_x represents the height of an interface above the substrate site x , Eq. (5) with $a = a^* = 2$ coincides with the growth equation proposed by Edwards and Wilkinson⁽⁶⁾ with unit surface tension ν , namely

$$\frac{\partial \varphi_x(t)}{\partial t} = \nu \nabla^2 \varphi_x(t) + \eta_x(t) \quad (22)$$

where ∇^2 is the discrete Laplacian defined as

$$\nabla^2 \varphi_x = \sum_{y(x)} (\varphi_y - \varphi_x) \quad (23)$$

Here the notation $y(x)$ means that the sum is restricted to the nearest neighbors of x . Then $W(L, t)$ coincides with the width of the interface, which, as a function of time and of the lateral extent of the substrate L , is found to exhibit the general scaling form⁽⁹⁾ $W(L, t) \propto L^\alpha f(t/L^z)$, which reduces to $W(L, t) \propto t^\beta$ for $t \ll L^z$ and to $W(L, t) \propto L^\alpha$ for $t \gg L^z$, where $\alpha = \beta z$ and z is the standard dynamical exponent.⁽¹¹⁾

For a d -dimensional substrate, Edwards and Wilkinson⁽⁶⁾ found $\beta = \max((2 - d)/4, 0)$ and $z = 2$ with an upper critical dimension of 2. Above $d = 2$ the interface is almost flat with $\alpha = \beta = 0$. Our results on a one-dimensional case thus coincide with the exact results. We shall now apply the same methodology to a nontrivial case.

2.2. Hierarchical Couplings

A rather interesting case which lacks translational invariance and which can be solved only by RG techniques is the case of a one-dimensional lattice where, however, the coupling between nearest neighbors is hierarchically distributed as in Fig. 1. In the case of diffusion, models of this kind have already been studied.^(10, 11)

In the present context we start from the modified Hamiltonian

$$H(\{\varphi\}) = \sum_x \frac{a_x}{2} \varphi_x^2 - \sum_{\langle xy \rangle} w_{x,y} \varphi_x \varphi_y \tag{24}$$

where $w_{x,y} = w_{y,x}$ have the hierarchical structure defined as follows (see Fig. 1):

$$w_{x,x-1} = w_{x-1,x} = \begin{cases} \varepsilon_n, & n \geq 1 \\ \varepsilon_0 = 1 \end{cases} \tag{25}$$

where $x = (2m + 1) 2^n$ ($n, m = 0, 1, 2, \dots$) and $w_{x,y} = 0$ if $|x - y| > 1$. The choice $\varepsilon_0 = 1$ can be made without loss of generality by a proper rescaling of the time scale.

As in the previous example, we will work at criticality. This corresponds to the choice $a_x = \sum_{y=x \pm 1} w_{x,y}$, i.e.,

$$H = \frac{1}{2} \sum_{\langle x,y \rangle} w_{x,y} (\varphi_x - \varphi_y)^2 \tag{26}$$

The implementation of the RG transformation closely follows the one used in the diffusion case^(10, 11) and it is based on the decimation of the sites indicated by circles in Fig. 1. Interestingly, due to the particular decimation scheme chosen, the minimal set of parameters for the variance which are invariant under RG transformation is $D_{x,y} = D_0 \delta_{x,y} + D_{1,2} \delta_{y,x \pm 1}$, where

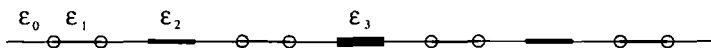


Fig. 1. Part of a one-dimensional lattice with hierarchical couplings between the nearest neighbors. Thicker bonds correspond to weaker coupling. Circled sites are eliminated after one RG step, which scales the system by a factor of 2.

one uses D_1 (D_2) if $w_{x,y} = \varepsilon_0$ (ε_n) respectively. In other words, a single self-correlation but two different nearest-neighbor correlations are involved. The recursions turn out to be

$$\hat{\phi}_{bx}(\omega, D) = A \frac{\alpha_1^2 - \varepsilon_1^2}{\varepsilon_1} \hat{\phi}_x(\omega', D') \quad (27a)$$

$$\varepsilon'_n = \varepsilon_{n+1} \frac{\alpha_1^2 - \varepsilon_1^2}{\varepsilon_1} \quad (n = 1, 2, \dots) \quad (27b)$$

$$\omega' = \frac{2(1 + 2\varepsilon_1)}{\varepsilon_1} \omega + O(\omega^2) \quad (27c)$$

$$A \hat{\eta}_{x'}(\omega') = \hat{\eta}_{x'}(\omega) + \frac{\hat{\eta}_{y_L}(\omega) \varepsilon_1 + \hat{\eta}_{y_R}(\omega) \alpha_1}{\alpha_1^2 - \varepsilon_1^2} \quad (27d)$$

where $\alpha_1 = -i\omega + 1 + \varepsilon_1$ and y_L (y_R) are left (right) sites which are decimated with respect to the barrier ε_1 . Apart from the noise contribution, the recursions are the same as in the case of diffusion.^(10, 11) It proves convenient to define $R_n = \varepsilon_{n+1}/\varepsilon_n$ since, upon iteration of Eq. (27a), it flows to a fixed point $R \in (0, 1]$ and then the analysis of the fixed points is reduced to a study of a two-dimensional map in the $\{\varepsilon_1, \omega\}$ plane. There are two fixed points $O = (\varepsilon_1^* = +\infty, \omega^* = 0)$ and $A = (\varepsilon_1^* = R/(1 - 2R), \omega^* = 0)$ whose stability depends upon the value of R . We will distinguish two cases:

(A) $R < 1/2$: A is stable and O is unstable and $y = d_w = \ln(2/R)/\ln 2$. The $\omega \rightarrow 0^+$ limit of the transition matrix T is

$$T = (2/R) A^{-2} \begin{Bmatrix} a(R) & b(R) & c(R) \\ c(R) & d(R) & e(R) \\ 0 & 0 & 1 \end{Bmatrix}$$

where $a(R) = 2(1 - R + R^2)$, $b(R) = 2(1 - R)$, $c(R) = 2R(1 - R)$, $d(R) = 2R$, $e(R) = 1 - 2R + 2R^2$. The value of A^* which yields a stable fixed line is $A^* = (4/R)^{1/2}$. Then, proceeding as in the previous example, one finds again

$$\alpha = \frac{y - 1}{2} = \frac{|\ln R|}{2 \ln 2}$$

as expected, since in this case $d_f = d = 1$.

(B) $R > 1/2$: O is stable and A is unstable and then $y = d_W = 2$ as in the equal-coupling case. The matrix T is

$$T = 4A^{-2} \begin{Bmatrix} \frac{3}{2} & 1 & \frac{1}{2} \\ \frac{1}{2} & 1 & \frac{1}{2} \\ 0 & 0 & 1 \end{Bmatrix}$$

which yields $A^* = 2^{3/2}$ (again as in the equal-coupling case) and consequently $\alpha = 1/2$.

3. FRACTALS

An interesting non-translationally invariant case which can be analyzed with the technique described above is the case of fractal structures. We will consider several examples which are prototypes of different physical situations.

3.1. Fractals with Uniform Coordination Numbers

The first example is the standard Sierpinski gasket shown in Fig. 2, whose fractal dimension is $d_f = \ln 3 / \ln 2$. In this case, as on translationally invariant structures, there is only one fixed point. The renormalization group procedure is readily implemented in the Fourier-transformed equation of motion (1) for the Hamiltonian (3), which reads

$$\alpha_x \hat{\phi}_x(\omega) = \sum_{y(x)} \hat{\phi}_y(\omega) + \hat{\eta}_x(\omega) \tag{28}$$

where $\alpha_x = a_x - i\omega$ and the sum is over nearest neighbors of x . The setup for the noise is the same as in the one-dimensional case. As before, we put

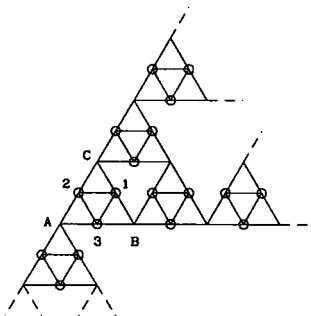


Fig. 2. Part of an infinite Sierpinski gasket in $d = 2$. Circled sites 1, 2, 3,... are eliminated in favor of surviving sites A, B, C, \dots after one RG step, which scales the system by a factor 2.

directly $a = a^* = 4$, corresponding to the static fixed point. Then, following standard procedure, the RG transformation is carried out in two steps:

(a) The $\hat{\phi}_x$ on the circled sites in Fig. 2 are eliminated in order to rescale the system by a scale factor b ($=2$ in this case). This may be done by solving Eq. (28) for $\hat{\phi}_x$ ($x = 1, 2, 3$) in terms of $\hat{\phi}_y$ ($y = A, B, C$) (see Fig. 2) and substituting the resulting equations back into (28).

(b) $\hat{\phi}_x$ and $\hat{\eta}_x$ are then suitably rescaled as follows:

$$\hat{\phi}_{bx}(\omega, D) = A(\omega + 6) \hat{\phi}_x(\omega', D') \tag{29a}$$

$$A\hat{\eta}_{x'}(\omega') = (\omega + 5)(\omega + 2) \hat{\eta}_{x'}(\omega) + 2 \sum_{y(x')} \hat{\eta}_y(\omega) + (\omega + 4) \sum_{y(x'')} \hat{\eta}_y(\omega) \tag{29b}$$

$$\omega' = \omega(5 - i\omega) \tag{29c}$$

where primed (unprimed) sites refer to the surviving (decimated) sites under the RG transformation, and $y(x)$ and $y(x'')$ are the decimated nearest neighbors and the decimated next nearest neighbors, respectively.

The procedure for calculating the amplitude A^* corresponding to the stable fixed point proceeds along exactly the same lines as the one-dimensional case: again the minimum set of parameters which are invariant under the RG transformation for the noise is $\{D_0, D_1\}$ corresponding to the self and nearest neighbor correlations, respectively. It is noteworthy that the presence of noise does *not* influence the renormalization of time, thus prompting the identification of the dynamical critical exponent z with the fractal dimension d_w of the walk on that structure giving the end-to-end distance $R(t)$ of the *ant in the labyrinth* at large t , i.e., $R(t) \sim t^{1/d_w}$. This is given by (29c) in the $\omega \rightarrow 0$ limit as $\omega' = b^{d_w}\omega$. One then finds the following critical exponents:

$$z = d_w, \quad \beta = \frac{2 - d_S}{4}, \quad \alpha = \frac{2 - d_S}{4} d_w = \frac{d_w - d_f}{2} \tag{30}$$

with $d_w = \ln 5 / \ln 2$ and $d_S = 2d_f / d_w = \ln 9 / \ln 5$ is the spectral dimension describing the low-frequency behavior of the density of vibrational modes.^(12, 13) A similar analysis can be carried out for a general d -dimensional Sierpinski gasket.

3.2. Fractals with Nonuniform Coordination Number

In the previous example we investigated the effect of the self-similarity of the structure on the scaling of the two-point correlation function for a

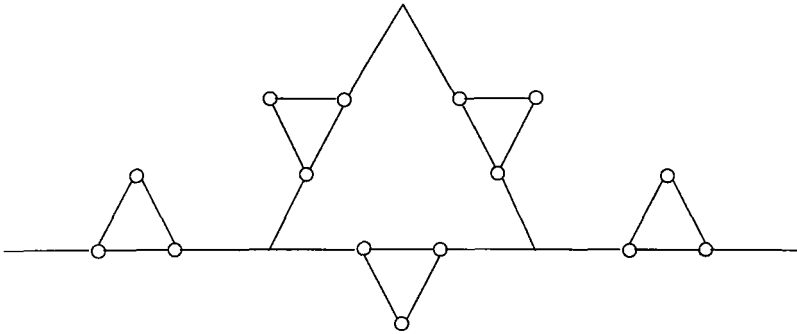


Fig. 3. Part of an infinite T-fractal in $d=2$, which has coordination numbers $z=1, 3$. Circled sites are eliminated after one RG step and this scales the system by a factor 2.

Langevin equation induced by a Gaussian Hamiltonian. However, in that example the coordination number was uniform (equal to 4) as in the translationally invariant lattice. The interplay between self-similarity of the substrate and nonuniformity of the coordination number has been recently investigated.⁽¹⁴⁾ Contrary to what happens on periodic structures, it has been shown that on both statistical and deterministic fractal structures the equilibrium properties of (3) are governed by two universality classes, corresponding to ideal polymers and to the ant in the labyrinth.⁽¹⁴⁾ We now study this effect on the Langevin equation on specific examples. The T-fractal (Fig. 3) has $z_x=1, 3$, whereas the branching Koch curve (BKC) (Fig. 4) has $z_x=2, 3$.

We stress again that the appearance of two fixed points is a feature of nonuniform coordination number and a fractal structure.

In the recursion relations we will derive below, the (minimum) set of parameters invariant under RG transformation is given by $D_{x,y}=D_{0z}$ if

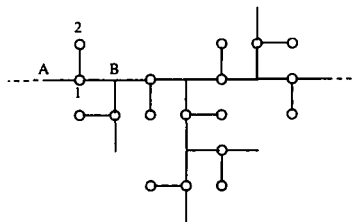


Fig. 4. Structure of the branching Koch curve in $d=2$, which has $z=2, 3$. Circled sites are eliminated after one RG step, which scales the system by a factor of 3.

$x = y$ (z is the coordination number), and $D_{x,y} = D_1$ if x and y are nearest neighbors and $D_{x,y} = 0$ otherwise. We will write

$$D = \begin{Bmatrix} D_{01} \\ D_{03} \\ D_1 \end{Bmatrix} \quad \text{and} \quad \alpha = \begin{pmatrix} \alpha_1 \\ \alpha_3 \end{pmatrix}$$

With this distinction in mind, calculations along the same lines as before yield the following recursions:

$$\hat{\phi}_{bx}(\alpha, D) = A \frac{\alpha_1 \alpha_3 - 1}{\alpha_1} \hat{\phi}_x(\alpha', D') \tag{31a}$$

$$A \hat{\eta}'_x(\alpha') = \hat{\eta}_x(\alpha) + \sum_{y(x)} [\alpha_1 \hat{\eta}_{y_1}(\alpha) + \hat{\eta}_{y_3}(\alpha)] / (\alpha_1 \alpha_3 - 1) \tag{31b}$$

and

$$\begin{aligned} \alpha'_1 &= \alpha_1 \alpha_3 - 2 \\ \alpha'_3 &= \alpha_3^2 - \alpha_3 / \alpha_1 - 3 \end{aligned} \tag{31c}$$

In the above definitions $\hat{\eta}_{y_1, y_3}$ represents the noise associated with sites of coordination 1 and 3, respectively.

In the static limit, $\omega = 0$, one has $\alpha_x = a_x$ and as found in ref. 14, the recursion equation (31c) admits two fixed points (see Fig. 5): $G = (a_1^*, a_3^*) = (1, 3)$, corresponding to the ant in the labyrinth, and $P = (a_1^*, a_3^*) = (\infty, (1 + \sqrt{13})/2)$, describing the scaling behavior of the ideal polymer.⁽¹⁴⁾ (The symbols G and P denote growth and polymer,

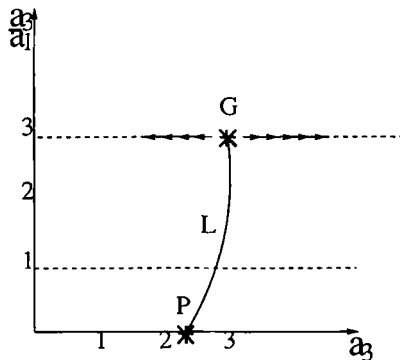


Fig. 5. Flow diagram for the RG analysis for the T-fractal example. Fixed points G and P correspond to *growth* and *polymer dynamic*, respectively. The line L is the critical line delimiting the unphysical region.

respectively.) Indeed, the linearized recursions (it is better to work with a_3 and a_3/a_1) show that G is unstable (two relevant eigendirections) with a thermal exponent $y_G = \ln 6/\ln 2$, which coincides with d_W ,^(12, 13) the random walk dimension, while P is stable (one relevant and one irrelevant eigendirection) with $y_P = \ln(1 + \sqrt{13})/\ln 2$ related to the end-to-end distance R of an ideal polymer of length N according to $N \sim R^{y_P}$.

Now let us turn to the dynamics. In the long-time limit, i.e., $\omega \rightarrow 0$, and near the above static fixed points one has $\alpha_x = a_x^*$. This implies that under renormalization ω rescales as $\omega(b) \sim b^y \omega$: thus the dynamical exponent z is equal to the thermal exponent y appropriate to the fixed point. From Eq. (31b) one can easily calculate the new noise correlation functions near the fixed point. The recursion equation is

$$D' = T \cdot D \tag{32}$$

with

$$T = 6A^{-2} \begin{pmatrix} \frac{3}{2} & \frac{1}{4} & \frac{1}{4} \\ \frac{3}{2} & \frac{5}{4} & \frac{1}{4} \\ \frac{9}{2} & \frac{3}{4} & \frac{7}{4} \end{pmatrix}$$

at the fixed point G and

$$T = 2a^{-1}A^{-2} \begin{pmatrix} 2a & 0 & a^2 \\ 2a & 1 & a^2 \\ 6a & 0 & 1 + 3a \end{pmatrix}$$

with $a^{-1} = (1 + \sqrt{13})/2$ at the fixed point C .

Thus, choosing the value of A so that the largest eigenvalue is 1, one finds that the corresponding eigenvector D^* is a stable fixed point. Near the fixed points, from Eq. (31a) one readily deduces the scaling of $\hat{\phi}_x(\omega, D^*)$ [we are writing $\hat{\phi}_x(\omega, D^*)$ instead of $\hat{\phi}_x(a^* - i\omega, D^*)$] in the $\omega \rightarrow 0$ limit:

$$\hat{\phi}_{bx}(\omega, D^*) = b^{\alpha+z} \hat{\phi}_x(b^z \omega, D^*) \tag{33}$$

From (31a) and (33), one finds ($b = 2$)

$$\alpha_G = \frac{y_G - d_f}{2} = \frac{1}{2} \quad \text{at } G, \quad \alpha_P = \frac{y_P - 1}{2} = 0.601... \quad \text{at } P \tag{34}$$

where $d_f = \ln 3/\ln 2$ is the fractal dimension of the structure. We will show below that the expression for α_G is completely general. Since $y_G = d_W$ and

the spectral dimension d_S describing the low-frequency behavior of the density of vibrational modes satisfies the scaling relation⁽¹³⁾ $d_S = 2d_f/d_w$, the result (34) for α_G can be rewritten as $\alpha_G = (2 - d_S)d_w/4$. Taking into account that $z = d_w$, one gets $\beta = (2 - d_S)/4$.

An extension of the T-fractals to sites with coordination $z = 1, 4$ leads to exactly the same expressions as before with the same numerical value of $\alpha_G = 1/2$ with a slightly higher value $\alpha_P = 0.678\dots$ for the other fixed point. Thus the α_G is the same as in the 1d model of Section 2.

A more interesting example, because it is a structure with loops, is the case of the branching Koch curve (see Fig. 4). Calculations in this case are rather tedious but quite analogous to the previous example and we will omit annoying details. Also in this case it is sufficient to start with a variance $D_{x,y} = D_{0z}\delta_{y,x} + D_1\delta_{|x-y|,1}$, where D_{0z} is defined as before and with two a 's, a_1 and a_2 , corresponding to two types of coordinations. At the fixed point $G = (a_2^* = 2, a_3^* = 3)$ one finds again $\alpha_G = (y_G - d_f)/2$ with $y_G = d_w = \ln(40/3)/\ln 3$ and $d_f = \ln 5/\ln 3$, consistent with the previous claim of a general form. The other fixed point $P = (a_2^* = +\infty, a_3^* = \sqrt{5})$ yields $y_P = \ln 11/\ln 3$ and $\alpha_P = \ln 2/\ln 3 = 0.6309\dots$. Notice that in the above example $\alpha_G \leq 1/2$, whereas $\alpha_P > 1/2$.

4. GENERALIZATIONS: GENERAL NETWORK AND NONLINEARITY

Equation (1) with $D_{xy} = D\delta_{xy}$ evolves to an equilibrium state with a probability distribution for $\{\varphi\}$ given by

$$\mathcal{P}_{\text{eq}}(\{\varphi\}) \propto \exp \left\{ \frac{-v}{2D} \sum_{\langle xy \rangle} (\varphi_x - \varphi_y)^2 \right\} \tag{35}$$

where x and y are nearest-neighbor sites.⁷ The equilibrium correlation function $\langle (\varphi_x - \varphi_0)^2 \rangle_T$ defined as in Eq. (19) calculated with the weight (35) can be shown⁽¹¹⁾ to be proportional to the resistance $\Omega_{x,0}$ between two fixed sites 0 and x of the fractal network where conductances (equal to v/D) connect nearest-neighbor sites, that is,

$$\langle (\varphi_x(t) - \varphi_0(t))^2 \rangle_T \sim \Omega_{x,0} \sim |x|^\zeta \tag{36}$$

where the last equality defines the exponent ζ for the resistivity. Scaling arguments predict that for fractals $\zeta = d_w - d_f$ (Einstein relation).⁽¹⁶⁾ Since

⁷ This can be deduced from the stationary solution of the Fokker-Planck equation associated with the Langevin equation (1); see any textbook on stochastic processes (e.g., ref. 15).

the roughness exponent α is defined by [see Eqs. (19), (20)] $\langle (\varphi_x - \varphi_0)^2 \rangle_T \sim |x|^{2\alpha}$, one finds $\alpha = (d_W - d_f)/2 = d_W(2 - d_S)/4$. On the basis of the previous exact RG, we argue that the ω renormalization [Eqs. (31) and (33)] is not influenced by the noise term in Eq. (1). We also note that Eq. (1) without the noise term is merely the diffusion equation with $\varphi_x(t)$ interpreted as the probability of finding a diffusing particle at x at time t . If ω renormalizes as $\omega' = b^z \omega$ to leading order, then the mean square distance traveled after time t behaves asymptotically like $t^{2/z}$,⁽¹¹⁾ implying $z = d_W$.

We now show that the temporal behavior of the width of the interface $W(t)$ for a substrate described by an arbitrary infinite network is also given by $t^{(2-d_S)/4}$ (provided that d_S can be defined⁽¹⁷⁾). This is a nontrivial result since we prove not only that the temporal growth has a power law form, but also obtain the exponent. The proof is heavily based on the rigorous results of Hattori *et al.*⁽¹⁸⁾ (HHW). We assume as initial condition $\varphi_x(t=0) = 0$. Let us go back to $G_{xy}(t) = \langle \varphi_x(t) \varphi_y(t) \rangle$, where the average is over the noise as defined in Section 1. The formal (forward) solution of Eq. (22) can be written as

$$\varphi_x(t) = \sum_y \int_0^t dt U_{xy}(t-t) \eta_y(t) \tag{37}$$

where $U_{x,y}(t)$ is the retarded Green function, associated with (22), satisfying

$$\left(\frac{\partial}{\partial t} - \nu \nabla_x^2 \right) U_{x,y}(t) = \delta_{x,y} \delta(t) \tag{38}$$

that is,

$$U_{x,y}(t) = \theta(t) (e^{t\nu \nabla_x^2})_{x,y} \tag{39}$$

where $\theta(\cdot)$ is the step function.

Using (38), we have

$$\begin{aligned} G_{x,x_0}(t) &= \langle \varphi_x(t) \varphi_{x_0}(t) \rangle = 2D \sum_y \int_0^t dt U_{x,y}(t-t) U_{x_0,y}(t-t) \\ &= 2D \int_0^t U_{x,x_0}(2(t-\tau)) \end{aligned} \tag{40}$$

where we have used the condition $\langle \eta_x(t_1) \eta_y(t_2) \rangle = 2D \delta_{x,y} \delta(t_1 - t_2)$.

Due to the initial condition $U_{x_0,x}(0^+) = \delta_{x_0,x}$, $G_{x,x_0}(t)$ is a solution of

$$\left(\frac{\partial}{\partial t} - 4D\nu \nabla_x^2 \right) G_{x,x_0}(t) = \delta_{x,x_0} 2D \tag{41}$$

It is then easy to verify that a probability $P_{x, x_0}(t)$ defined through

$$G_{x, x_0}(t) = \int_0^{4Dt} d\tau P_{x, x_0}(\tau) \tag{42}$$

is a solution of the diffusion equation

$$\left(\frac{\partial}{\partial t} - \nu \nabla_x^2\right) P_{x, x_0}(t) = 0 \tag{43}$$

The results of ref. 18 can now be applied to Eq. (42) defined on the sites of an arbitrary graph. Since, under very general conditions, $P_{x_0, x_0}(t) \sim t^{-d_S/2}$, from Eq. (42) we get

$$W^2(L, t)|_{L=\infty} = G_{x_0, x_0}(t) \sim t^{2\beta} \tag{44}$$

where $\beta = (2 - d_S)/4$ as expected from the previously solved cases.

From the same procedure one can recover also the exponent α . Indeed if we assume the standard *ansatz* which appears to be valid for a generic fractal,⁽¹⁹⁾

$$P_{x, x_0}(t) = \frac{1}{t^{d_S/2}} \Phi(t |x - x_0|^{-\nu}) \tag{45}$$

and using Eqs. (42) and (44), one finds $W(L, t) = L^\alpha f(t/L^z)$ with $\alpha = d_W(2 - d_S)/4$ as before (for α_G and $z = y$).

We now turn to nonlinear growth on a fractal. We conjecture that the analog of the nonlinear growth equation of ref. 20 is given by

$$\frac{\partial \varphi_x(t)}{\partial t} = \nu \sum_{y(x)} [\varphi_y(t) - \varphi_x(t)] + \lambda \sum_{y(x)} [\varphi_y(t) - \varphi_x(t)]^2 + \eta_x(t) \tag{46}$$

where now $\varphi_x(t)$ is to be interpreted as the height of the substrate at position x at time t . The λ term takes into account the lateral growth of the aggregate.⁽²⁰⁾ When $\lambda = 0$ we recover Eq. (22). Under rescaling of a factor b of the length, the left-hand side and the first two terms of the right-hand side scale as $b^{\alpha-z}$, $b^{\alpha-d_W}$, and $b^{2\alpha-d_W}$, respectively, where b^{-d_W} comes from the Laplacian on a fractal.⁸ In the absence of the λ term, dimensional analysis yields $z = d_W$ (found above), whereas the presence of the λ term leads to the time derivative on the left-hand side balancing the λ term:

$$\alpha + z = d_W \tag{47}$$

⁸ Since on an infinite lattice $\sum_x \varphi_x(t) \sum_{y(x)} [\varphi_y(t) - \varphi_x(t)] = -\sum_x \sum_{y(x)} [\varphi_y(t) - \varphi_x(t)]^2$, the scalings of the first two terms on the r.h.s. of Eq. (46) differ by a factor b^α (scaling of φ).

with the ν term being subdominant. Equation (47) generalizes the exact equation^(23, 24) for Euclidean lattices which are characterized by $d_w = 2$.

Additionally, following ref. 21, if we identify the dimension of the noise term to be $b^{-(z+d_f)/2}$ (this is expected to hold in the linear case where the λ term is absent) and extending the dimensional analysis, we find again Eq. (34) for α_G .

In the presence of the λ term, one may conjecture that the noise term scales as $b^{-(z+\alpha d_c)/2}$, where d_c is the chemical dimension of the fractal.⁽²²⁾ With this *ad hoc* assumption one finds for Eq. (46)

$$z = d_w \frac{2 + d_c}{3 + d_c}, \quad \beta = \frac{1}{2 + d_c}, \quad \alpha = \frac{d_w}{3 + d_c} \tag{48}$$

leading to $\alpha = 0.5064$, $\beta = 0.2789$ in $d=2$, and $\alpha = 0.5170$, $\beta = 0.2500$ in $d=3$ Sierpinski gaskets. [For the gaskets in d dimensions $d_c = d_f = \ln(d+1)/\ln 2$ and $d_w = \ln(d+3)/\ln 2$.⁽¹³⁾]

We stress the fact that Eqs. (47) and (48) have been derived simply on the basis of power counting, and reduce to previously known approximations on translationally invariant structures.^(21, 22)

5. NUMERICAL ANALYSIS

In order to verify Eq. (47) and check the conjecture leading to Eq. (48), we have carried out computer simulations of growth models on Sierpinski gaskets. We considered a sequence of sizes of gaskets in both two and three dimensions, the largest one containing 1095 and 2050 sites, respectively. The value of α was estimated by comparing the scaling of the saturated roughness with system size, whereas β was deduced by studying the temporal dependence of the roughness for the larger sizes [i.e., $W(L, t) \sim L^\alpha$ for $t \gg L^z$ and $W(L, t) \sim t^\beta$ for $t \ll L^z$].

To check the correctness of the programs, we first studied the linear growth process in both $d=2$ and 3 by adding and subtracting particles on the gasket sites with the same probability and found excellent agreement with the exact results of Eq. (34).

The nonlinear case was then studied by carrying out simulations of the Kim-Kosterlitz⁽²²⁾ growth model for the gaskets; the numerical results confirmed the validity of Eq. (47). Specifically we found $\alpha = 0.48 \pm 0.02$ and $\beta = 0.26 \pm 0.02$ in $d=2$, whereas $\alpha = 0.48 \pm 0.02$ and $\beta = 0.23 \pm 0.02$ in $d=3$.

6. DISCUSSION AND CONCLUSION

Our discussion so far has been restricted to growth on fractal substrates with the particles arriving along a space dimension orthogonal to

that in which the fractal resides. One might also consider growth on a self-affine substrate (with no overhangs, so that all sites are accessible to the incoming particles) with the growth occurring in the direction normal to the rough surface, but yet in the d -dimensional hyperplane in which the surface resides. In this case, the resulting growth would be characterized by the regular exponents in $d-1$ dimensions. This follows readily from two observations:

(i) The exponent α characterizing the growth is a measure of the equilibrium roughness and does not depend on whether the initial configuration is a self-affine or a planar interface.

(ii) It is reasonable that the exponent z which may be defined by studying the relaxation of small perturbations around equilibrium is typically the same that characterizes the approach to equilibrium from any initial configuration.

The exponent β is deduced directly from α and z . Thus the growth exponents in this case are trivially determined.

Another observation is noteworthy. The results given here are valid for systems of continuous symmetry spins where, to the best of our knowledge, no analog of Henley's argument, valid for Ising spins undergoing Glauber dynamics,⁽²⁵⁾ is known.

In conclusion, we have presented a complete analysis of linear Langevin dynamics. The analysis has been carried out in real space and is based on a combinations of RG analysis, rigorous results, and heuristic considerations.

The primary results of our dynamical RG analysis are:

1. For Eq. (22), i.e., for linear⁽⁶⁾ growth processes, the width of the interface grows algebraically with time and the exponent $\beta = (2 - d_S)/4$, where d_S is the spectral dimension of the substrate. We stress that it is not common to demonstrate explicitly in a rigorous way such a power law behavior. Indeed, this result is valid not only for a fractal substrate, but for any generic substrate: d_S can be rigorously defined⁽¹⁸⁾ for almost⁽¹⁷⁾ all infinite graphs consisting of a set of nodes and links joining sites that are defined to be nearest neighbors.

2. For a fractal substrate, $z = d_W$, and $\alpha = (2 - d_S)d_W/4$, where d_W is the random walk dimension characterizing the asymptotic behavior of the root mean square distance R traveled after a time t , $R \sim t^{1/d_W}$ (d_W , d_S , and the fractal dimension d_f are related by $d_S = 2d_f/d_W$ ^(26, 12)).

3. For both fixed points of the Hamiltonian (3) the dynamical exponent z coincides with the thermal critical exponent γ of the corresponding static problem.

Result 1 is rigorous, while results 2 and 3 are based on exact arguments. For the nonlinear growth model (46), heuristic arguments and numerical analysis suggest that Eqs. (48) and (49) are at least good approximations.

ACKNOWLEDGMENTS

This work was supported by grants from NASA, NATO, NSF, ONR, the Donors of the Petroleum Research Fund administered by the American Chemical Society, and the Center for Academic Computing at Penn State.

NOTE ADDED IN PROOF

It must be noticed that Langevin equation (1), with the Hamiltonian (3) and a noise correlated over nearest-neighbor sites as in Eq. (11), leads to an equilibrium distribution: $\mathcal{P}(\{\varphi\}) \propto \exp[-\tilde{H}(\{\varphi\})]$, where the Hamiltonian \tilde{H} contains interactions which are short ranged, but not limited to nearest-neighbor sites as in H .

It may be proved that the static correlation functions corresponding to H and \tilde{H} exhibit the same long range behavior.

REFERENCES

1. P. C. Hohenberg and B. I. Halperin, *Rev. Mod. Phys.* **49**:435 (1977), and references therein.
2. S. K. Ma, *Modern Theory of Critical Phenomena* (Addison-Wesley, Reading, Massachusetts, 1976).
3. G. F. Mazenko, In *Dynamical Critical Phenomena and Related Topics*, C. D. Enz, ed. (Springer-Verlag, New York, 1979).
4. S. K. Ma and G. F. Mazenko, *Phys. Rev. B* **11**:4077 (1975).
5. P. G. de Gennes, *Recherche* **7**:919 (1976).
6. S. F. Edwards and D. R. Wilkinson, *Proc. R. Soc. Lond. A* **381**:17 (1982).
7. J. W. Haus and K. W. Kehr, *Phys. Rep. C* **150**:263 (1987).
8. A. Maritan, F. Toigo, and J. R. Banavar, Department of Physics, University of Padua. Internal Report (INFMI-1994).
9. F. Family and T. Vicsek, *J. Phys. A* **18**:175 (1985).
10. B. Hubermann and M. Kerszberg, *J. Phys. A* **19**:L331 (1985); S. Teitel and E. Domany, *Phys. Rev. Lett.* **55**:2176 (1985); A. Maritan and A. L. Stella, *J. Phys. A* **19**:L269 (1986).
11. A. Giacometti, A. Maritan, and A. L. Stella, *Int. J. Mod. Phys.* **5**:709 (1991).
12. S. Alexander and A. Orbach, *J. Phys. Lett.* (Paris) **43**:L625 (1982).
13. R. Rammal and G. Toulouse, *J. Phys. Lett.* (Paris) **44**:L13 (1983).
14. A. Maritan, *Phys. Rev. Lett.* **62**:2845 (1989); A. Giacometti, H. Nakanishi, A. Maritan, and N. H. Fuchs, *J. Phys. A* **25**:L461 (1992); A. Giacometti, A. Maritan, and H. Nakanishi, *J. Stat. Phys.* **75**:669 (1994).
15. C. W. Gardiner, *Handbook of Stochastic Methods* (Springer-Verlag, Berlin, 1990).
16. Y. Gefen, A. Aharony, and E. Alexander, *Phys. Rev. Lett.* **50**:77 (1983).
17. D. Cassi, *Int. J. Mod. Phys. B* **6**:85 (1992).

18. K. Hattori, T. Hattori, and H. Watanabe, *Progr. Theor. Phys. Suppl.* **92**:108 (1987).
19. S. Havlin and D. Ben-Abraham, *Adv. Phys.* **36**:695 (1987).
20. M. Kardar, G. Parisi, and Y.-C. Zhang, *Phys. Rev. Lett.* **56**:889 (1986).
21. H. G. E. Hentschel and F. Family, *Phys. Rev. Lett.* **66**:1982 (1991).
22. J. M. Kim and J. M. Kosterlitz, *Phys. Rev. Lett.* **62**:2289 (1989).
23. P. Meakin, P. Ramanlal, L. M. Sander, and R. C. Ball, *Phys. Rev. A* **34**:5091 (1986).
24. D. Forster, D. R. Nelson, and M. J. Stephen, *Phys. Rev. A* **16**:732 (1989).
25. C. Henley, *Phys. Rev. Lett.* **54**:2030 (1985); D. Kutasov, E. Domany, and E. Pytte, *Phys. Rev. B* **35**:3354 (1987).
26. D. Dhar, *J. Math. Phys.* **18**:577 (1977).